Published in final edited form as:

J Mol Cell Cardiol. 2016 September ; 98: 138–145. doi:10.1016/j.yjmcc.2016.05.014.

Mesenchymal Stem Cells Suppress Cardiac Alternans by Activation of PI3K Mediated Nitroso-Redox Pathway

Prasongchai Sattayaprasert[1,2], **Drew M Nassal**[2], **Xiaoping Wan**[2], **Isabelle Deschenes**[2], and **Kenneth R Laurita**[2]

[1]Department of Internal Medicine, MetroHealth Campus of Case Western Reserve University, Cleveland, Ohio

[2]Heart & Vascular Research Center, MetroHealth Campus of Case Western Reserve University, Cleveland, Ohio

Abstract

Background—The paracrine action of non-cardiac progenitor cells is robust, but not well understood. Mesenchymal stem cells (MSC) have been shown to enhance calcium (Ca^{++}) cycling in myocytes. Therefore, we hypothesized that MSCs can suppress cardiac alternans, an important arrhythmia substrate, by paracrine action on Ca^{++} cycling.

Methods and Results—Human cardiac myocyte monolayers derived from iPS cells (hCM) were cultured without or with human MSCs (hMSC) directly or plated on a transwell insert. Ca^{++} transient alternans (Ca^{++} ALT) and Ca^{++} transient duration (CaD) were measured from hCM monolayers following application of 200 µM H_2O_2. Ca^{++} ALT in hCM was significantly decreased when cultured with hMSCs directly (97%, $p<0.0001$) and when cultured with hMSC in the transwell insert (80%, $P<0.0001$). When hCM with hMSCs were pretreated with PI3K or eNOS inhibitors, Ca^{++} ALT was larger than baseline by 20% ($p<0.0001$) and 36% ($p<0.0001$), respectively. In contrast, Ca^{++} ALT was reduced by 89% compared to baseline ($p<0.0001$) when hCM monolayers without hMSCs were pretreated with 20 µM GSNO. In all experiments, changes in Ca^{++} ALT were mirrored by changes in CaD. Finally, real time quantitative PCR revealed no significant differences in mRNA expression of RyR2, SERCA2a, and phospholamban between hCM cultured with or without hMSCs.

Conclusion—Ca^{++} ALT is suppressed by hMSCs in a paracrine fashion due to activation of a PI3K-mediated nitroso-redox pathway. These findings demonstrate, for the first time, how stem cell therapy might be antiarrhythmic by suppressing cardiac alternans through paracrine action on Ca^{++} cycling.

Address Correspondence to: Kenneth R. Laurita, Ph.D., Heart and Vascular Research Center, MetroHealth Campus, Case Western Reserve University, 2500 MetroHealth Drive, Rammelkamp, 6th floor, Cleveland, OH 44109-1997, TEL: (216) 778-7340, FAX: (216) 778-1261, Kenneth.Laurita@case.edu.

Disclosures

There are no conflicts of interest to disclose.

Keywords

Mesenchymal Stem cells; Alternans; Oxidative Stress; Arrhythmia; SERCA2a

1. Introduction

Cell base therapy for cardiac disease continues to generate significant clinical and experimental interest. Among the many cell types considered, non-cardiac progenitor cells (e.g. adult bone marrow cells) have been investigated in numerous experimental studies and clinical trials. Their modest efficacy of improved cardiac function [1-3], reduced scar size [1-4], and improved functional status [1, 3-5] have been shown repeatedly in clinical trials. Other than pro-arrhythmia concerns raised primarily from *in vitro* studies [6-8], *in vivo* experiments and clinical trials using mesenchymal stem cells (MSC) do not increase ventricular tachycardia or other indices related to prognosis and ventricular arrhythmia occurrence [4, 5, 9-12]. Several clinical trials have even shown a decrease in arrhythmias [3, 13-15]. For example, Hare, *et al* [15] have shown fewer PVCs and VT in patients that received MSC therapy, and in a recent meta-analysis bone marrow cell therapy reduced arrhythmia incidence [3]. Despite such results, the mechanisms of any electrophysiological benefit associated with non-cardiac progenitor cells is hard to realize given limited electrical integration and the inability to transdifferentiate into cardiac myocytes. This has led to the belief that any electrophysiological benefit of non-cardiac progenitor cells must be largely indirect or by paracrine signaling, however such mechanisms are not well understood.

The paracrine action of non-cardiac progenitor cells is well recognized [16-18]. Valle-Prieto *et al* [19] showed a cytoprotective effect due to anti-oxidant properties of non-cardiac progenitor cells. More recently, DeSantiago *et al* [20] showed the benefit of MSCs to protect against cardiomyocyte cell death via Akt phosphorylation and activation of the endothelial nitric oxide synthase (eNOS) pathway [20]. Specifically, they show that MSCs improved Ca^{++} cycling by increasing SERCA2a function. Dysregulation of Ca^{++} handling is a known mechanism of cardiac alternans [21-25]. Furthermore, abnormal SERCA2a function has been closely associated with cardiac alternans, an important determinant of arrhythmogenesis in disease [26, 34]. Therefore we hypothesize that MSCs can suppress cardiac alternans, by paracrine action on intracellular Ca^{++} cycling.

2. Material and Methods

2.1. Cell isolation and culture

Human cardiac myocytes derived from induced pluripotent stem cells (hCM) were purchased from Cellular Dynamics Inc. [27-29]. Cell pellets in the cryoprecipitate tube were thawed and cultured as monolayers on 25 mm diameter cover slips according to the protocol provided by the manufacturer. Culture media was changed every 2 days, until day 14-20 when experiments were performed.

Human mesenchymal stem cells (hMSC) were isolated from bone marrow aspirates and purified at the Case Comprehensive Cancer Center Hematopoietic Biorepository and

Cellular Therapy Core using protocol previously described [30]. Briefly, human bone marrow was aspirated from the posterior iliac crest of a healthy human volunteer donor under an approved Institutional Review Board protocol. The cell suspension was washed with hMSC growth medium, consisting of low glucose DMEM (DMEM-LG; Sigma/Aldrich, St. Louis, MO) supplemented with 1% antibiotic–antimycotic solution (Invitrogen), 1% GlutaMAX (Invitrogen), and 10% hMSC-tested FBS (Sigma/Aldrich, St. Louis, MO). Mononuclear cells were separated using a Percoll gradient (Sigma/Aldrich). The cell suspension was plated at 6×10^5 cell per T-150 tissue culture flask in hMSC growth medium, supplemented with 10 ng/ml fibroblast growth factor-2 (FGF-2, R&D Systems, Minneapolis, MN). Culture and incubation were performed in a humidified, 95% air/5% CO_2 environment at 37°C. Media was gently changed every 3 days, until spindle cell colonies became dense. Cells were then detached using 0.25% trypsin-ethylenediaminetetraacetic acid (EDTA, 1 mmol/L; Invitrogen), and subcultured in a new flask to eliminate trypsin resistant cells. Cells were cultured to passage 3-5 and then plated on 25 mm diameter cover slips (with hCM) or transwell-plates (see experimental groups below).

2.2. Experimental Protocol

Experiments were divided into 3 groups where hCM monolayers were cultured alone (hCM), co-cultured with hMSC (hCM+hMSC) in direct contact, or cultured with hMSC in a transwell plate insert (hCM+$hMSC_{trans}$) with a pore diameter of (0.4 μm) to assess paracrine action. Before they were co-cultured with hCM, hMSC were stained with Dil cell tracker (Sigma/Aldrich). Cell density of hMSCs was titrated at 500 (1%), 2500 (5%), and 10000 (20%) cells per 50000 of hCM for hCM+hMSC and hCM+$hMSC_{trans}$ groups, corresponding to percentages previously reported [8]. All cultures with hMSCs were maintained for 2 days before performing any experiments. Transwell inserts were removed just before experiments were performed.

For Ca^{++} recordings, monolayers were incubated with Tyrodes solution (140 NaCl, 4.56 KCl, 0.73 $MgCl_2$, 10 HEPES, 5.0 dextrose, 1.25 $CaCl_2$) containing 5 μM Fluo-3AM (Sigma/Aldrich) for 20 minutes. Monolayers were then washed with normal Tyrodes solution before mounting on a bath chamber designed for field stimulation. The chamber was mounted on a stage adapter and Fluo-3AM fluorescence (485/530 nm) was measured using an inverted Axiovert fluorescence microscope (Zeiss) with a cooled CCD camera (Princeton Instruments) over a 420 μm by 320 μm field of view. Additionally, DiI fluorescence was measured (553/570 nm) to confirm hMSC presence. Ca^{++} transients were measured from hCM in an area without hMSCs. In several experiments, APD was measured in these monolayers by staining with di-4-ANEPPS (10 μM) for 20 minutes. In a sub group, hMSC and hCM were plated at a very high density of 60,000 and 300,000 cells (20%), respectively, for imaging over a large area (16 mm by 12 mm). In all groups, cells were paced at a cycle length of 750 msec for only measuring alternans and 1200 msec for only measuring Ca^{++} transient duration. Hydrogenperoxide (H_2O_2) was then added at 200 μM and pacing and recordings were repeated. All experiments were performed at room temperature.

To determine signaling mechanisms, Wortmannin (PI3K Inhibitor; Santa Cruz Biotechnology) or LY294002 (PI3K Inhibitor; Sigma/Ald) were used to inhibit the Akt pathway. Wortmannin (100 nmol/L) or LY294002 (10 μM) were incubated at the time of co-culture for 2 days, and continued throughout the experiment. To determining downstream nitroso-redox signaling pathways, the eNOS inhibitor (L-NIO dihydrochloride; Sigma/Aldrich) was used by incubating at 10 μM for 20 minutes before and during an experiment. Finally, an NO donor (GSNO) was prepared at 20 μM before the experiment and added to the cell culture. For each treatment tested, separate control experiments (no treatment) were always performed.

2.3. Patch clamp recordings

Patch-clamp recordings in current clamp mode were carried out in the whole-cell configuration at body temperature (35°C) to measure APD. Transmembrane potential was recorded from isolated hCM using perforated patch with an Axopatch 200B amplifier (Axon Instruments, Foster City, CA, USA). Briefly, the cells were bathed in a chamber continuously perfused with Tyrode's solution composed of (mmol/L) NaCl 137, KCl 5.4, $CaCl_2$ 2.0, $MgSO_4$ 1.0, Glucose 10, HEPES 10, pH to 7.35 with NaOH. Patch pipettes (Corning Kovar Sealing code 7052, WPI) were pulled from borosilicate capillary glass and lightly fire-polished to resistance 0.9-1.5 MΩ when filled with electrode solution composed of (mmol/L) aspartic acid 120, KCl 20, NaCl 10, $MgCl_2$ 2, HEPES 5, and 24 μg/ml of amphotericin-B (Sigma, St. Louis, MO), pH7.3. A gigaseal was rapidly formed. Typically, 10 minutes later, amphotericin-B pores lowered the resistance sufficiently to current clamp the cells. Myocytes were paced in the current clamp mode using a 1.5 - 2 diastolic threshold 5 msec current pulse at 1 Hz. Command and data acquisition were operated with an Axopatch 200B patch clamp amplifier controlled by a personal computer using a Digidata 1200 acquisition board driven by pCLAMP 7.0 software (Axon Instruments, Foster City, CA).

2.4. Real Time Reverse Transcriptase Polymerase Chain Reaction

Total RNA from hCM was isolated using Trizol reagent (Invitrogen) according to the manufacturer's instructions, and subsequently DNAase treated using a Qiagen RNAeasy on-column DNase digestion. Purified RNA was used as a template for cDNA synthesis in reverse transcriptase reactions using the Multiscribe Reverse Transcription kit (Invitrogen) and primed with Random Hexamers (Roche). The quantitative PCR reactions were performed using the ABI 7500 Real-Time PCR system with Power SYBR Green PCR Master Mix (Invitrogen). Relative expression was calculated using the ΔΔCt-method with normalization to GAPDH expression. RT-PCR was performed using primers for RYR2 (F: AAG TGC CAG AGT CAG CAT TC; R: AGT AGT ATC CAA TGA TGC AG), SERCA2a (F: GAG AAC GCG CAC ACC AAG A; R: TTG GAG CCC CAT CTC TCC TT), Phospholamban (F: ACT TCA GAC TTC CTG TCC TGC; R: CGT GCT TGT TGA GGC ATT TCA), and GAPDH (F: TCC TCT GAC TTC AAC AGC GA; R: GGG TCT TAC TCC TTG GAG GC).

2.5. Data Analysis

Ca^{++} transient alternans (Ca^{++} ALT) was recorded at a pacing cycle length of 750 msec and calculated as the difference in amplitude between two consecutive beats normalized to the amplitude of the larger transient as described previously [21]. The Ca^{++} transient duration (CaD) was measured while pacing at a constant cycle length of 1200 msec and calculated as the duration at half peak amplitude. For each monolayer tested, recordings and analysis were repeated three times and averaged. Then, this average was averaged across all monolayers within a group and reported as mean±SEM. Two-tailed paired t-tests and unpaired t-test were used as appropriate and statistical significance was defined as $p < 0.05$.

3. Results

Ca^{++} transients were recorded from hCM monolayers in the absence of hMSCs (hCM group) at baseline and then during acute administration of H_20_2 to increased oxidative stress, as may occur in disease conditions. Pacing at a CL of 750 msec was used to induce Ca^{++} ALT. Ca^{++} transients shown in Figure 1 (left) demonstrate Ca^{++} ALT under baseline conditions (black) that increase markedly with the administration of H_20_2 (red). The traces below show Ca^{++} transients recorded at a slower pacing CL (1200 msec) in the absence of Ca^{++} ALT from which Ca^{++} transient duration (CaD) was measured, which also increased with H_20_2. Ca^{++} ALT was also observed at 36°C, occurred during steady state conditions, and exhibited rate dependence (Figure 2, Supplemental Material). Over all experiments, a highly significant increase in Ca^{++} ALT (132.2 %) and CaD (9.8 %) was observed with oxidative stress. Furthermore, hCM monolayers exhibit a predominant effect of the SR on Ca^{++} cycling as indicated by significant attenuation of Ca^{++} transient amplitude with Ryanodine and Thapsigargin (Figure 1B), evidence of Ca^{++} sparks (Figure 1, Supplemental Material), and the inhibitory effect of Isoproterenol on Ca^{++} ALT (Figure 3, Supplemental Material). These findings are not new for cardiac myocytes in general, rather they are meant to establish our model for the remainder of the study.

To determine the effect of hMSCs on hCM during oxidative stress, hCM monolayers were co-cultured with hMSCs in direct contact (hCM+hMSC group) for 2 days and then exposed to H_20_2 as described above. Shown in Figure 2 (top left) is a representative image of an hCM +hMSC co-culture where all cells are stained with the Ca^{++} indicator Fluo-3AM (green), but only hMSCs were pre-stained with DiI (orange). Ca^{++} transient recordings were always performed from a region void of hMSCs (see box). Representative traces show that Ca^{++} ALT measured from hCM co-cultured with hMSCs (hCM+hMSC) is much less (largely absent) compared to hCM alone. Summary data show that hMSCs essentially eliminated Ca^{++} ALT (right top). In addition, CaD (right bottom) was significantly reduced when hCM were co-cultured with hMSCs, compared to hCM alone (traces not shown). Several densities of hMSCs were tested and shown to have a dose dependent effect on Ca^{++} ALT when co-cultured with hCM (Figure 3). In particular, at 10000 hMSC per 50,000 hCM, Ca^{++} ALT was essentially eliminated. Finally, we repeated some experiments using more densely plated cells over a much larger area (16 × 12 mm). Activation times, approximated from the time of 50% Ca^{++} release, reveled a conduction velocity (14±1 cm/sec) comparable to that measured in well coupled monolayers using hCM from the same provider [28]. Figure 4, shows that with hCM alone Ca^{++} ALT is present throughout the entire mapping field. Furthermore, Ca^{++} ALT is spatially discordant. However, when hCM were co-cultured with hMSCs, Ca^{++} ALT was significantly reduced with no evidence of spatial discordance. Summary data (Figure 4C) show that hMSC significantly reduced Ca^{++} ALT uniformly over large regions, which is similar to that observed over smaller regions at a high resolution (Figure 2). These results suggest that hMSCs have a causal and significant impact on the suppression of Ca^{++} ALT in hCM monolayers.

In a co-culture, it is possible that the action of hMSCs is by direct contact with hCM (e.g. an electrotonic effect) or by paracrine action. To test this, hCM were cultured with hMSCs in a transwell insert (hCM+$hMSC_{trans}$) for the same duration and at the highest cell density as the hMSC co-cultures. Transwell plates were removed before Ca^{++} transient recordings and the administration of H_20_2. Subsequent results are shown with H_20_2 present. As demonstrated by representative traces in Figure 5 (left), Ca^{++} ALT in hCM+$hMSC_{trans}$ (bottom) was reduced compared to hCM alone (top). Similar results for Ca^{++} ALT were observed over all experiments (Figure 5, right). Furthermore, media conditioned with hMSCs also significantly decreased Ca^{++} ALT (0.20±0.04 au, $p < 0.0003$). Notably, Ca^{++} ALT in hCM+$hMSC_{trans}$ (grey bar) was not reduced to the same level as when hCM were co-cultured in direct contact with hMSCs (black bar). Nevertheless, the magnitude of Ca^{++} ALT was reduced significantly below hCM alone and even below hCM alone under baseline conditions (no H_2O_2, Figure 1, 0.25±0.05 au). Similar findings were observed with CaD. These data suggest that the reduction of Ca^{++} ALT by hMSCs is, largely, by paracrine action.

APD alternans (APD ALT) was also reduced in hCM+$hMSC_{trans}$ compared to hCM alone (Figure 6A), indicating that the suppression of alternans by hMSC is electrical as well. Shown are action potentials measured from hCM (left) and hCM+$hMSC_{trans}$ (right) monolayers while pacing at 1200 msec (top) and 750 msec (bottom) cycle lengths. At 750 msec pacing cycle length, significant APD alternans is observed only in hCM monolayers as demonstrated in the examples shown and summary data. In addition, PCR analysis (Figure 6B) showed no difference in SERCA2a, Phospholamban, and RyR2 message in hCM alone compared to hCM+$hMSC_{trans}$. Finally, action potential amplitude, APD90, APD50, and RMP measured in hCM isolated from co-cultures with hMSCs in the absence of H_2O_2 (109±3 mV, 328±22 msec, 214±19 msec,−61±2 mV, respectively), were no different from that measured in isolated hCM that were cultured alone (100±6 mV, 325±24 msec, 222±24 msec, −56±2 mV, respectively) suggesting no persistent effect on repolarization currents and membrane potential (n=10 for both groups). Taken together, these data suggest that Ca^{++} ALT is reduced in hCM cultured with hMSCs by a mechanism unrelated to expression of Ca^{++} cycling proteins or repolarization currents that may shorten APD.

Previously it has been shown in mouse myocytes that MSCs can enhance Ca^{++} regulation through the PI3K/Akt signaling pathway. Experiments were performed to test if this same pathway is responsible for reduced Ca^{++} ALT and CaD in human cells (Figure 7). Ca^{++} recordings were compared with and without wortmannin or LY294002 to inhibit PI3K. With wortmannin (+WORT) or LY294002 (+LY), Ca^{++} ALT in hCM+$hMSC_{trans}$ was significantly increased compared to hCM+$hMSC_{trans}$ with no treatment (left, gray bar). To test downstream eNOS signaling, the eNOS inhibitor L-NIO significantly increased Ca^{++} ALT in hCM+$hMSC_{trans}$ (+L-NIO) similar to PI3K inhibition. Finally, the NO donor GSNO, added to hCM cultured without hMSCs, significantly reduced Ca^{++} ALT to a level similar as hCM+$hMSC_{trans}$. GSNO may activate multiple ionic currents (e.g. I_{Ks}) such that the net effect is to shorten APD and, thus, reduce alternans independent of the SR. In separate experiments, GSNO tended to shorten APD measured in hCM monolayers compared to control (−5%, p=0.1); however, this did not reach significance. This may, nonetheless, explain why GSNO had the greatest effect on Ca^{++} ALT (Figure 7). However, as in isolated cells, hMSCs had little effect on APD measured in hCM monolayers (3% increase, p=0.27). Under all conditions, changes in CaD paralleled Ca^{++} ALT (Figure 7, right). These findings suggest that hMSCs can suppress Ca^{++} ALT in a paracrine fashion mediated by PI3K/Akt activation of nitroso-redox regulation of Ca^{++} signaling.

Finally, it is possible that activation of the PI3K/Akt pathway modulates RyR function, which can also influence Ca^{++} ALT. We compared Ca transient time to peak (Tp) under the same experimental conditions that CaD was measured. Shown in Figure 8 are representative Ca^{++} transients measured from hCM co-cultured with (hCM+hMSC) and without (hCM) hMSCs. In this example, Tp is increased alongside CaD in the absence of hMSCs, but on average the change in CaD (218 msec) is much greater than Tp (74 msec). In fact, when average Tp and CaD were correlated under all conditions tested, a significant positive correlation was observed (right). Moreover, because the slope of this relationship (2.4) is much greater than unity, suggests that increased CaD is not merely due to an increase in Tp. Therefore, the close correlation between CaD and Tp indicates that, as shown previously under conditions of oxidative stress [31], changes in Ca^{++} uptake drive SR Ca^{++} load which, in turn, drives Ca^{++} release.

4. Discussion

The electrophysiological benefit of stem cell therapy is questionable given limited electrical integration and availability of cells with a suitable electrophysiological phenotype. Even when electrical integration is proven to be robust, cardiac myocytes derived from embryonic stem cells can be pro-arrhythmic [32]. Non-cardiac progenitor cells *in vitro*, such as MSCs, can directly attenuate impulse conduction velocity when co-cultured with normal cardiac myocytes [8]. However, in most clinical trials MSCs have been shown to be safe and exhibit anti-arrhythmic behavior [3, 15]. Yet, non-cardiac progenitor cells are unlikely to directly contribute to electrical activity by generating action potentials [33]. In general, the paracrine action of stem cells is known to be strong [18], but such action on electrophysiology and arrhythmia substrates is not well known. In this study we demonstrate that hMSCs reduce cardiac alternans in human cardiac myocytes by paracrine action. Specifically, this is secondary to the PI3K/Akt signaling pathway that activates eNOS and, in turn, accelerates Ca^{++} cycling.

4.1. Mechanism of paracrine action on alternans suppression

Previously, we [26, 34] and others [22, 23, 35] have shown that abnormal Ca^{++} regulation is an important mechanism of arrhythmias, especially under disease conditions. In the present study, we show that hMSCs accelerate Ca^{++} cycling in cardiac myocytes and reduce Ca^{++} and APD alternans (Figure 2, 6). Alternatively, shortening of APD (e.g. increased repolarization kinetics) can decrease APD alternans that can, in turn, decrease Ca^{++} alternans by action of membrane potential on intracellular Ca^{++} (i.e. Vm-to-Ca coupling). Thus, it is possible that hMSCs shorten APD, which could then explain the reduction of Ca^{++} alternans that we observed. However, we found that hMSCs had no persistent effect on hCM APD and resting membrane potential. Additionally, it has been shown in previous studies that non-excitable cells (like MSCs) prolong APD of cardiac myocytes [36, 37] which should increase alternans. Others [9] have shown that MSCs can shorten APD when co-cultured long term with rat cardiac myocytes by reverse remodeling of repolarization currents. This could also explain a decrease in alternans, but not our observations because this was only seen after 6 days of co-culture, which is much longer than the time we cultured hMSCs with cardiac myocytes (2 days). Thus, hMSCs can reduce alternans by accelerating Ca^{++} cycling.

4.2. Mechanisms of paracrine action on Ca^{++} regulation

Our findings suggest that the mechanism of alternans suppression is by action on the function of SR Ca^{++} regulatory proteins that govern Ca^{++} cycling. We found no change in RyR2, SERCA2a, and PLN mRNA, so it is unlikely that changes in protein expression (e.g. increased SERCA2a) can explain our result (Figure 6). De Santiago *et al* [20] previously showed that MSCs increase $I_{Ca,L}$ in addition to SERCA2a function by paracrine action. The increase in $I_{Ca,L}$ is unlikely to explain our results because, if anything, this should increase alternans since block of $I_{Ca,L}$ decreases alternans [38-40]. Finally, it is possible that increased RyR2 function can explain the decrease in alternans that we observed. We found that Tp was decreased with hMSCs, suggesting that RyR2 function was increased. However, when Tp was correlated with CaD under all conditions tested (Figure 8) we found a strong positive correlation with a slope >> 1. This suggests two things. First, the changes in CaD cannot be explained by changes in Tp. Second, it is well known that changes in SERCA2a function and thus, SR Ca^{++} load, can indirectly affect Ca^{++} release. A strong positive correlation between CaD and Tp might be expected if oxidative stress is acting mostly on SERCA2a as demonstrated previously [31]. However, we cannot rule out the possibility that activation of PI3K/Akt signaling has some direct action on RyR2 to suppress alternans. It is beyond the scope of the current manuscript to pinpoint this mechanism.

It is important to discuss the mechanisms that may link PI3K/Akt/eNOS activation with increased SERCA2a function. Given the localization of eNOS to the sarcolemma, it may not induce a direct effect such as S-nitrosylation; alternatively, the signaling may be through the cGMP/PKG pathway. Yet, our results with GSNO and those reported by others [41] suggest that direct S-nitrosylation is associated with accelerated Ca^{++} decay. Since models of nitrosoredox imbalance exhibit slower Ca^{++} decay [42], and there is evidence that phosphorylation and S-nitrosylation of phospholamban are required for activation of SERCA2a [43], suggests an important role of S-nitrosylation and restoring nitroso-redox balance.

We can only speculate on the exact paracrine signaling molecules involved. Exosomes from stems cells have recently been shown to exert potent effects on host cardiac myocytes [18]. In addition, MSCs have been associated with numerous secretory factors [44]. It's possible that these may activate the PI3K/Akt pathway. For example, it is possible that a cytokine from MSCs, such as IGFBP-2 [44, 45], VEGF [20, 46, 47], or HASF [48] activate the PI3K/Akt pathway.

4.3. Direct versus paracrine action of MSCs on alternans

It is interesting to point out that while hMSCs cultured in the transwell are able to largely reduce alternans below baseline by paracrine action, this effect was not as great as hMSCs in direct contact (Figure 5). This suggests some additional suppression of alternans by direct contact. For example, it's known that non-excitable cells *in vitro* electrically coupled to cardiac myocytes and can alter RMP and APD. However, the reported effect is a prolongation of APD in cardiac myocytes by electrotonic loading [37]. However, such APD prolonging effect was only observed at cell ratios much higher than what we used and only in cells engineered to express connexin 43. More importantly, the APD prolonging effect would, as mentioned above, increase alternans not decrease alternans. Thus, based on these previous reports we cannot explain why alternans suppression was increased with cells in direct contact. Alternatively, if the suppression of alternans is solely by paracrine action, then it is possible that a larger gradient of signal was present when cells were in direct contact compared to being in the transwell insert.

4.4. Clinical implications

Our results may have important clinical implications. Non-cardiac progenitor cells have been shown to be safe and provide some therapeutic benefit [3]. Yet, their direct electrophysiological action is limited since they are unlikely to actively propagate action potential activity [33], and electrical integration is not robust. However, such direct action may not be necessary for significant electrophysiological benefit, as we show. Other studies have shown proarrhythmic nature of MSCs *in vitro* and we don't dispute these results. Nevertheless, in those previous studies MSCs were co-cultured with normal cardiomyocytes, which may not be the actual clinical setting. For example, we have previously shown that when MSCs are infused at the time of injury arrhythmia vulnerability is decreased [49], and when MSCs are directly injected into borderzone tissue impulse conduction slowing is reduced [50]. Moreover, as suggested in the present study paracrine action may also lessen Ca^{++} mediated arrhythmia substrates such as alternans, which are heightened in the infarct border zone [26, 51].

4.5. Limitations

CM derived from iPS cells have an immature phenotype in regard to Ca^{++} cycling. However, we demonstrate that alternans in CM derived from iPS cells exhibits many of the characteristic of that measured in adult cells such as a strong dependence on heart rate and SR Ca^{++} reuptake. Thus it is possible that only the magnitude of MSC paracrine action may be different when cultured with adult cardiac myocytes. Finally, we did not test a variety of stem cell types, but it is likely that such paracrine action is associated with other non-cardiac and cardiac progenitor cells.

Supplementary Material

Refer to Web version on PubMed Central for supplementary material.

Acknowledgments

We thank Anna D Dikina and Dr. Eben Alsberg from the Departments of Orthopedic Surgery and Biomedical Engineering, Case Western Reserve University, Cleveland, Ohio for providing the human mesenchymal stem cells.

Sources of funding

This material is based upon work supported by NIH grants HL123012 (KRL), and NIH grants HL-094450 and HL-096962 (ID).

References

1. Karantalis V, DiFede DL, Gerstenblith G, Pham S, Symes J, Zambrano JP, et al. Autologous mesenchymal stem cells produce concordant improvements in regional function, tissue perfusion, and fibrotic burden when administered to patients undergoing coronary artery bypass grafting: The Prospective Randomized Study of Mesenchymal Stem Cell Therapy in Patients Undergoing Cardiac Surgery (PROMETHEUS) trial. Circ Res. 2014; 114:1302–10. [PubMed: 24565698]
2. Suncion VY, Ghersin E, Fishman JE, Zambrano JP, Karantalis V, Mandel N, et al. Does Transendocardial Injection of Mesenchymal Stem Cells Improve Myocardial Function Locally or Globally?: An Analysis From the Percutaneous Stem Cell Injection Delivery Effects on Neomyogenesis (POSEIDON) Randomized Trial. Circ Res. 2014; 114:1292–301. [PubMed: 24449819]
3. Afzal MR, Samanta A, Shah ZI, Jeevanantham V, Abdel-Latif A, Zuba-Surma EK, et al. Adult Bone Marrow Cell Therapy for Ischemic Heart Disease: Evidence and Insights from Randomized Controlled Trials. Circ Res. 2015
4. Heldman AW, DiFede DL, Fishman JE, Zambrano JP, Trachtenberg BH, Karantalis V, et al. Transendocardial mesenchymal stem cells and mononuclear bone marrow cells for ischemic cardiomyopathy: the TAC-HFT randomized trial. JAMA : the journal of the American Medical Association. 2014; 311:62–73. [PubMed: 24247587]
5. Hare JM, Fishman JE, Gerstenblith G, DiFede Velazquez DL, Zambrano JP, Suncion VY, et al. Comparison of allogeneic vs autologous bone marrow-derived mesenchymal stem cells delivered by transendocardial injection in patients with ischemic cardiomyopathy: the POSEIDON randomized trial. Jama. 2012; 308:2369–79. [PubMed: 23117550]
6. Askar SF, Ramkisoensing AA, Atsma DE, Schalij MJ, de Vries AA, Pijnappels DA. Engraftment patterns of human adult mesenchymal stem cells expose electrotonic and paracrine proarrhythmic mechanisms in myocardial cell cultures. Circ Arrhythm Electrophysiol. 2013; 6:380–91. [PubMed: 23420831]
7. Price MJ, Chou CC, Frantzen M, Miyamoto T, Kar S, Lee S, et al. Intravenous mesenchymal stem cell therapy early after reperfused acute myocardial infarction improves left ventricular function and alters electrophysiologic properties. Int J Cardiol. 2006; 111:231–9. [PubMed: 16246440]
8. Chang MG, Tung L, Sekar RB, Chang CY, Cysyk J, Dong P, et al. Proarrhythmic potential of mesenchymal stem cell transplantation revealed in an in vitro coculture model. Circulation. 2006; 113:1832–41. [PubMed: 16606790]
9. Cai B, Wang G, Chen N, Liu Y, Yin K, Ning C, et al. Bone marrow mesenchymal stem cells protected post-infarcted myocardium against arrhythmias via reversing potassium channels remodelling. Journal of cellular and molecular medicine. 2014
10. Yang Z, Zhang F, Ma W, Chen B, Zhou F, Xu Z, et al. A novel approach to transplanting bone marrow stem cells to repair human myocardial infarction: delivery via a noninfarct-relative artery. Cardiovasc Ther. 2010; 28:380–5. [PubMed: 20337639]
11. Straburzynska-Migaj E, Popiel M, Grajek S, Katarzynska-Szymanska A, Lesiak M, Breborowicz P, et al. Exercise capacity, arrhythmic risk profile, and pulmonary function is not influenced by

intracoronary injection of bone marrow stem cells in patients with acute myocardial infarction. Int J Cardiol. 2012; 159:134–8. [PubMed: 21392832]

12. Ascheim DD, Gelijns AC, Goldstein D, Moye LA, Smedira N, Lee S, et al. Mesenchymal precursor cells as adjunctive therapy in recipients of contemporary left ventricular assist devices. Circulation. 2014; 129:2287–96. [PubMed: 24682346]
13. Wang Y, Xue M, Xuan YL, Hu HS, Cheng WJ, Suo F, et al. Mesenchymal stem cell therapy improves diabetic cardiac autonomic neuropathy and decreases the inducibility of ventricular arrhythmias. Heart Lung Circ. 2013; 22:1018–25. [PubMed: 23850388]
14. Katritsis DG, Sotiropoulou P, Giazitzoglou E, Karvouni E, Papamichail M. Electrophysiological effects of intracoronary transplantation of autologous mesenchymal and endothelial progenitor cells. Europace. 2007; 9:167–71. [PubMed: 17272327]
15. Hare JM, Traverse JH, Henry TD, Dib N, Strumpf RK, Schulman SP, et al. A randomized, double-blind, placebo-controlled, dose-escalation study of intravenous adult human mesenchymal stem cells (prochymal) after acute myocardial infarction. J Am Coll Cardiol. 2009; 54:2277–86. [PubMed: 19958962]
16. Kim C, Majdi M, Xia P, Wei KA, Talantova M, Spiering S, et al. Non-cardiomyocytes influence the electrophysiological maturation of human embryonic stem cell-derived cardiomyocytes during differentiation. Stem Cells Dev. 2010; 19:783–95. [PubMed: 20001453]
17. Zhang Y, Liang X, Liao S, Wang W, Wang J, Li X, et al. Potent Paracrine Effects of human induced Pluripotent Stem Cell-derived Mesenchymal Stem Cells Attenuate Doxorubicin-induced Cardiomyopathy. Sci Rep. 2015; 5:11235. [PubMed: 26057572]
18. Khan M, Nickoloff E, Abramova T, Johnson J, Verma SK, Krishnamurthy P, et al. Embryonic Stem Cell-Derived Exosomes Promote Endogenous Repair Mechanisms and Enhance Cardiac Function Following Myocardial Infarction. Circ Res. 2015; 117:52–64. [PubMed: 25904597]
19. Valle-Prieto A, Conget PA. Human mesenchymal stem cells efficiently manage oxidative stress. Stem Cells Dev. 2010; 19:1885–93. [PubMed: 20380515]
20. DeSantiago J, Bare DJ, Semenov I, Minshall RD, Geenen DL, Wolska BM, et al. Excitation-contraction coupling in ventricular myocytes is enhanced by paracrine signaling from mesenchymal stem cells. J Mol Cell Cardiol. 2012; 52:1249–56. [PubMed: 22465692]
21. Pruvot EJ, Katra RP, Rosenbaum DS, Laurita KR. Role of calcium cycling versus restitution in the mechanism of repolarization alternans. Circ Res. 2004; 94:1083–90. [PubMed: 15016735]
22. Goldhaber JI, Xie LH, Duong T, Motter C, Khuu K, Weiss JN. Action potential duration restitution and alternans in rabbit ventricular myocytes: the key role of intracellular calcium cycling. Circ Res. 2005; 96:459–66. [PubMed: 15662034]
23. Clusin WT. Mechanisms of calcium transient and action potential alternans in cardiac cells and tissues. Am J Physiol Heart Circ Physiol. 2008; 294:H1–H10. [PubMed: 17951365]
24. Kanaporis G, Blatter LA. The mechanisms of calcium cycling and action potential dynamics in cardiac alternans. Circ Res. 2015; 116:846–56. [PubMed: 25532796]
25. Eisner DA, Choi HS, Diaz ME, O'Neill SC, Trafford AW. Integrative analysis of calcium cycling in cardiac muscle. Circ Res. 2000; 87:1087–94. [PubMed: 11110764]
26. Plummer BN, Liu H, Wan X, Deschenes I, Laurita KR. Targeted antioxidant treatment decreases cardiac alternans associated with chronic myocardial infarction. Circ Arrhythm Electrophysiol. 2015; 8:165–73. [PubMed: 25491741]
27. Ma J, Guo L, Fiene SJ, Anson BD, Thomson JA, Kamp TJ, et al. High purity human-induced pluripotent stem cell-derived cardiomyocytes: electrophysiological properties of action potentials and ionic currents. Am J Physiol Heart Circ Physiol. 2011; 301:H2006–17. [PubMed: 21890694]
28. Lee P, Klos M, Bollensdorff C, Hou L, Ewart P, Kamp TJ, et al. Simultaneous voltage and calcium mapping of genetically purified human induced pluripotent stem cell-derived cardiac myocyte monolayers. Circ Res. 2012; 110:1556–63. [PubMed: 22570367]
29. Fine M, Lu FM, Lin MJ, Moe O, Wang HR, Hilgemann DW. Human-induced pluripotent stem cell-derived cardiomyocytes for studies of cardiac ion transporters. Am J Physiol Cell Physiol. 2013; 305:C481–91. [PubMed: 23804202]
30. Love Z, Wang F, Dennis J, Awadallah A, Salem N, Lin Y, et al. Imaging of mesenchymal stem cell transplant by bioluminescence and PET. J Nucl Med. 2007; 48:2011–20. [PubMed: 18006616]

31. Greensmith DJ, Eisner DA, Nirmalan M. The effects of hydrogen peroxide on intracellular calcium handling and contractility in the rat ventricular myocyte. Cell Calcium. 2010; 48:341–51. [PubMed: 21106236]
32. Chong JJ, Yang X, Don CW, Minami E, Liu YW, Weyers JJ, et al. Human embryonic-stem-cell-derived cardiomyocytes regenerate non-human primate hearts. Nature. 2014; 510:273–7. [PubMed: 24776797]
33. Costa AR, Panda NC, Yong S, Mayorga ME, Pawlowski GP, Fan K, et al. Optical mapping of cryoinjured rat myocardium grafted with mesenchymal stem cells. Am J Physiol Heart Circ Physiol. 2012; 302:H270–7. [PubMed: 22037193]
34. Cutler MJ, Wan X, Plummer BN, Liu H, Deschenes I, Laurita KR, et al. Targeted sarcoplasmic reticulum Ca2+ ATPase 2a gene delivery to restore electrical stability in the failing heart. Circulation. 2012; 126:2095–104. [PubMed: 23019291]
35. Balijepalli RC, Lokuta AJ, Maertz NA, Buck JM, Haworth RA, Valdivia HH, et al. Depletion of T-tubules and specific subcellular changes in sarcolemmal proteins in tachycardia-induced heart failure. Cardiovasc Res. 2003; 59:67–77. [PubMed: 12829177]
36. Pedrotty DM, Klinger RY, Kirkton RD, Bursac N. Cardiac fibroblast paracrine factors alter impulse conduction and ion channel expression of neonatal rat cardiomyocytes. Cardiovasc Res. 2009; 83:688–97. [PubMed: 19477968]
37. McSpadden LC, Kirkton RD, Bursac N. Electrotonic loading of anisotropic cardiac monolayers by unexcitable cells depends on connexin type and expression level. Am J Physiol Cell Physiol. 2009; 297:C339–C51. [PubMed: 19494239]
38. Hashimoto H, Suzuki K, Miyake S, Nakashima M. Effect of calcium antagonists on the electrical alternans of the ST segment during acute coronary occlusion in dogs. Jpn Heart J. 1981; 22:247–56. [PubMed: 7230524]
39. Nearing BD, Hutter JJ, Verrier RL. Potent antifibrillatory effect of combined blockade of calcium channels and 5-HT_2 receptors with nexopamil during myocardial ischemia and reperfusion in dogs: Comparison to diltiazem. JCardiovascPharmacol. 1996; 27:777–87.
40. Mahajan A, Sato D, Shiferaw Y, Baher A, Xie LH, Peralta R, et al. Modifying L-type calcium current kinetics: consequences for cardiac excitation and arrhythmia dynamics. Biophys J. 2008; 94:411–23. [PubMed: 18160661]
41. Hatzistergos KE, Paulino EC, Dulce RA, Takeuchi LM, Bellio MA, Kulandavelu S, et al. SNitrosoglutathione Reductase Deficiency Enhances the Proliferative Expansion of Adult Heart Progenitors and Myocytes Post Myocardial Infarction. J Am Heart Assoc. 2015:4.
42. Dulce RA, Yiginer O, Gonzalez DR, Goss G, Feng N, Zheng M, et al. Hydralazine and organic nitrates restore impaired excitation-contraction coupling by reducing calcium leak associated with nitroso-redox imbalance. J Biol Chem. 2013; 288:6522–33. [PubMed: 23319593]
43. Irie T, Sips PY, Kai S, Kida K, Ikeda K, Hirai S, et al. S-Nitrosylation of Calcium-Handling Proteins in Cardiac Adrenergic Signaling and Hypertrophy. Circ Res. 2015; 117:793–803. [PubMed: 26259881]
44. Wagner W, Roderburg C, Wein F, Diehlmann A, Frankhauser M, Schubert R, et al. Molecular and secretory profiles of human mesenchymal stromal cells and their abilities to maintain primitive hematopoietic progenitors. Stem Cells. 2007; 25:2638–47. [PubMed: 17615262]
45. Shen X, Xi G, Wai C, Clemmons DR. The coordinate cellular response to insulin-like growth factor-I (IGF-I) and insulin-like growth factor-binding protein-2 (IGFBP-2) is regulated through vimentin binding to receptor tyrosine phosphatase beta (RPTPbeta). J Biol Chem. 2015; 290:11578–90. [PubMed: 25787077]
46. Gnecchi M, Zhang Z, Ni A, Dzau VJ. Paracrine mechanisms in adult stem cell signaling and therapy. Circ Res. 2008; 103:1204–19. [PubMed: 19028920]
47. Chen XG, Lv YX, Zhao D, Zhang L, Zheng F, Yang JY, et al. Vascular endothelial growth factor-C protects heart from ischemia/reperfusion injury by inhibiting cardiomyocyte apoptosis. Mol Cell Biochem. 2016; 413:9–23. [PubMed: 26769665]
48. Beigi F, Schmeckpeper J, Pow-Anpongkul P, Payne JA, Zhang L, Zhang Z, et al. C3orf58, a novel paracrine protein, stimulates cardiomyocyte cell-cycle progression through the PI3K-AKT-CDK7 pathway. Circ Res. 2013; 113:372–80. [PubMed: 23784961]

49. Mills WR, Mal N, Kiedrowski MJ, Unger R, Forudi F, Popovic ZB, et al. Stem cell therapy enhances electrical viability in myocardial infarction. J Mol Cell Cardiol. 2007; 42:304–14. [PubMed: 17070540]

50. Panda NC, Zuckerman ST, Mesubi OO, Rosenbaum DS, Penn MS, Donahue JK, et al. Improved conduction and increased cell retention in healed MI using mesenchymal stem cells suspended in alginate hydrogel. J Interv Card Electrophysiol. 2014; 41:117–27. [PubMed: 25234602]

51. Lou Q, Efimov IR. Enhanced susceptibility to alternans in a rabbit model of chronic myocardial infarction. Conf Proc IEEE Eng Med Biol Soc. 2009; 2009:4527–30. [PubMed: 19964643]

Research highlights

- Human mesenchymal stem cells suppress cardiac alternans measured in human cardiac myocytes in the setting of oxidative stress.
- Suppression of cardiac alternans by mesenchymal stem cells is, largely, paracrine in nature.
- The mechanism of cardiac alternans suppression by mesenchymal stem cells is activation of a PI3K-mediated nitroso-redox pathway that improves Ca^{++} cycling.

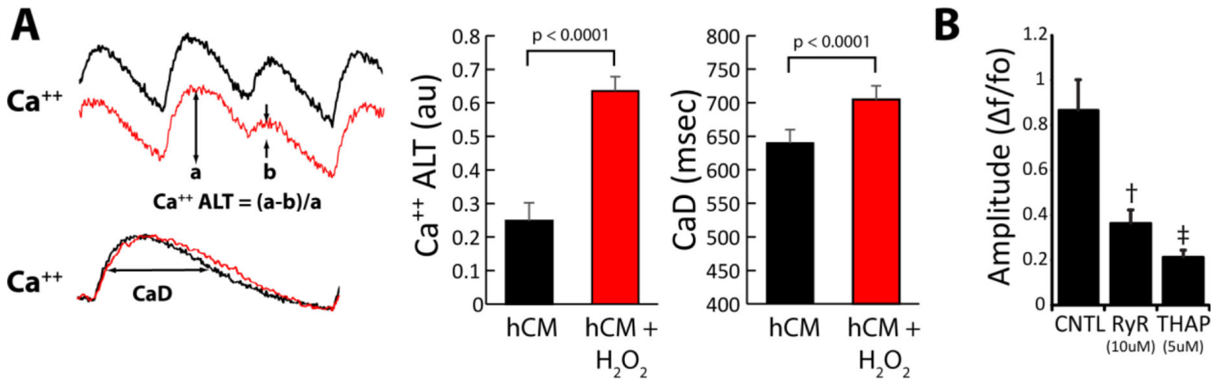

Figure 1.

Panel A shows the effects of oxidative stress (H_2O_2, 200 μM) on hCM. Ca^{++} transient recordings (left) show an increase in Ca^{++} ALT and CaD under conditions of oxidative stress (H_2O_2). Graphs (right) show summary data before and after H_2O_2 at 200 μM where oxidative stress significantly increased Ca^{++} ALT (n=13, $p< 0.001$) and CaD (n=8, $p<0.0001$). Panel B shows the inhibitory effect of Ryanodine (RyR, 10 μM) and Thapsigargin (THAP, 5 μM) on Ca^{++} transient amplitude († = $p< 0.01$, ‡ = $p< 0.0001$, compared to CNTL, n=7).

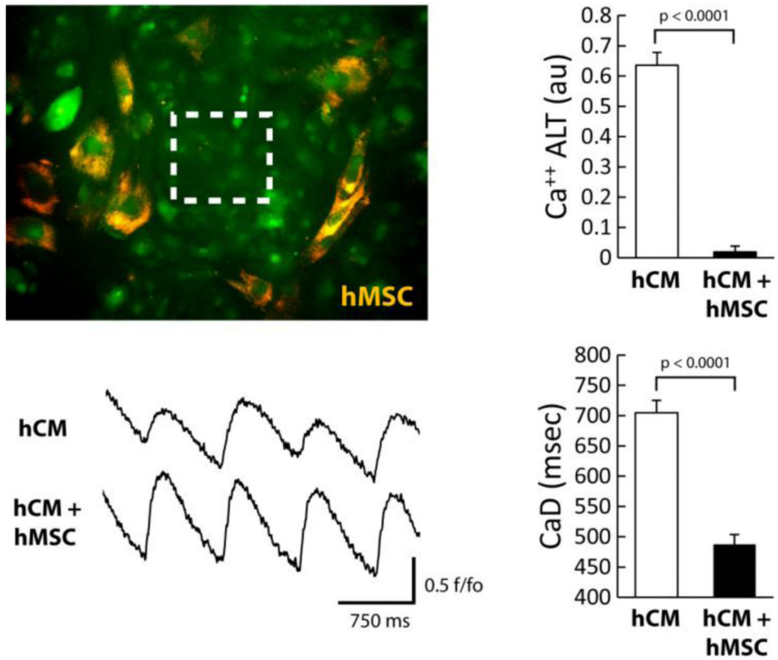

Figure 2.

Image of hCM monolayer co-cultured directly with hMSC (orange). Ca^{++} transients were recorded from a region indicated by the white box. The effects of hMSC (10000 cells) on hCM under conditions of oxidative stress are shown. Ca^{++} transient recordings in the presence of H_2O_2 (left) show a decrease in Ca^{++} ALT with hMSC compared to hCM alone. The graphs (right) show summary data for hCM alone or with hMSC. Overall, hMSC significantly decreased Ca^{++} ALT (n=9, $p< 0.0001$) and CaD (n=8, $p<0.0001$).

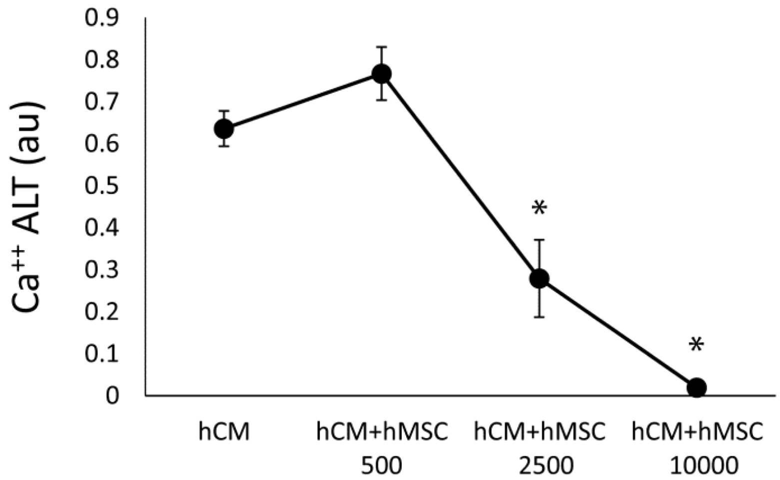

Figure 3.

Dose response of hMSC co-cultured with hCM. Under oxidative stress conditions, increasing dose of hMSC monotonically decreased Ca^{++} ALT. Co-culture with 2500 hMSC and 10000 hMSC per 50000 hCM showed significant decrease in Ca^{++} ALT compared to hCM alone (n=6, * $p < 0.0001$).

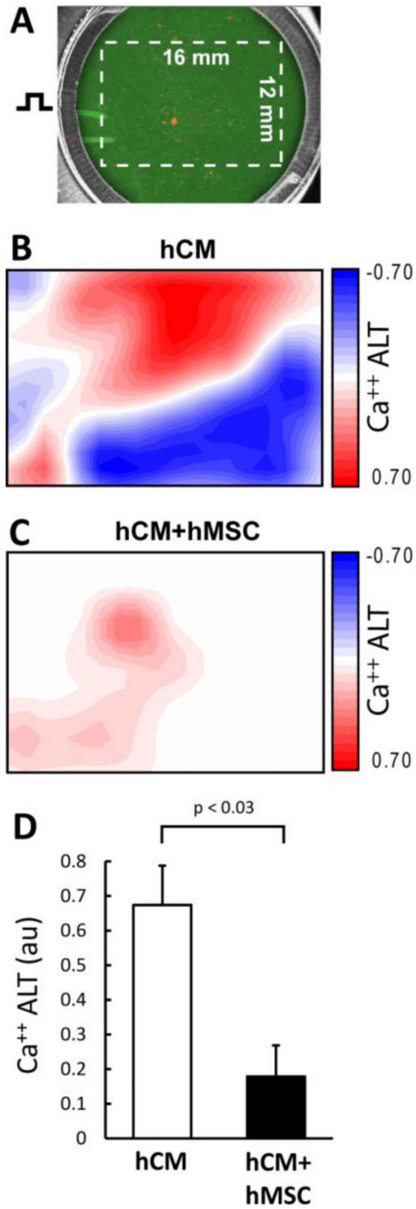

Figure 4.

Ca^{++} ALT measured from a large, high density hCM monolayer (Panel A) co-cultured with hMSC (50,000 hMSC per 300,000 hCM). During point stimulation at 750 msec cycle length, significant Ca^{++} ALT is present. Red and blue contours indicate Ca^{++} ALT in opposite phase (spatially discordant alternans). When co-cultured with hMSC, Ca^{++} ALT is almost completely eliminated (Panel C). Summary data (Panel D) show that hMSC significantly reduced Ca^{++} ALT in large high density monolayers (n=3).

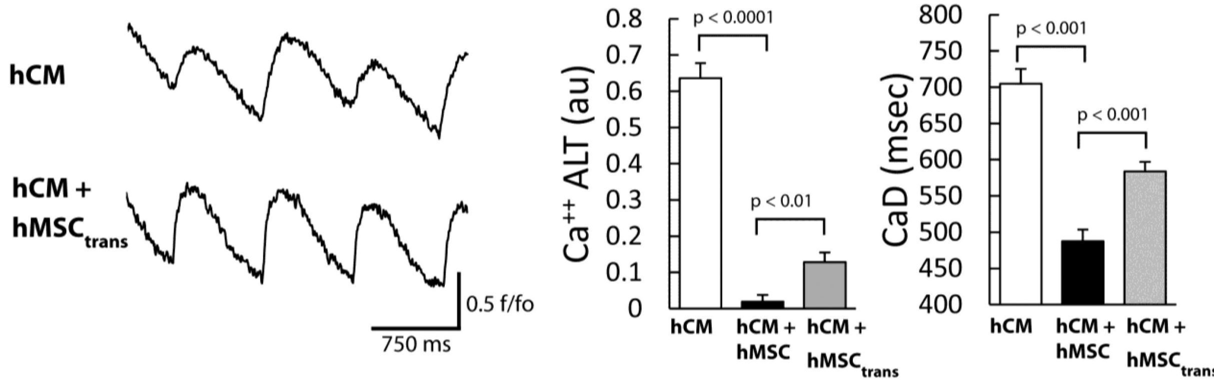

Figure 5.

The effects of hMSC indirectly co-cultured (via transwell) with hCM (hCM+hMSC$_{trans}$). Ca^{++} transient recordings in the presence of H_2O_2 (left) show a decrease in Ca^{++} ALT for hCM+hMSC$_{trans}$ (bottom) compared to hCM alone (top). The graphs (right) show summary data for hCM alone (white bar), hCM+hMSC$_{trans}$, (gray bar) and hCM+hMSC (black bar, repeated for comparison). Overall, hCM+hMSC$_{trans}$, significantly decreased Ca^{++} ALT (n=6, $p< 0.0001$) and CaD (n=6, $p<0.001$). Ca^{++} ALT in hCM+hMSC$_{trans}$ was not reduced to the same level as when hCM were co-cultured in direct contact with hMSC.

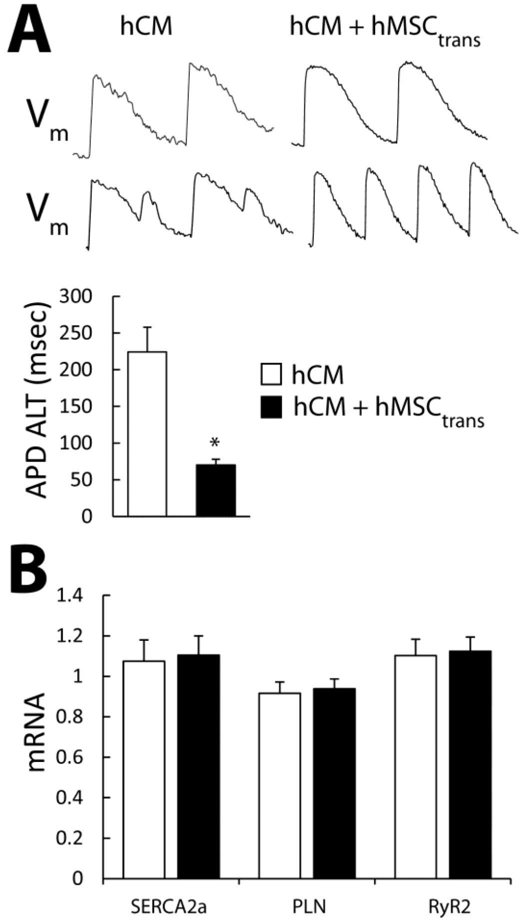

Figure 6.

Panel A shows example of action potential alternans measured in hCM (left) and hCM +hMSC$_{trans}$ (right). APD ALT (APD long beat – APD short beat) is significantly ($p < 0.003$, n=6) decreased in hCM+hMSC$_{trans}$ compared to hCM alone (graph). No difference in SERCA2a, Phospholamban, and RyR2 mRNA expression (Panel B) are observed in hCM alone compared to hCM+hMSC$_{trans}$ (n=3).

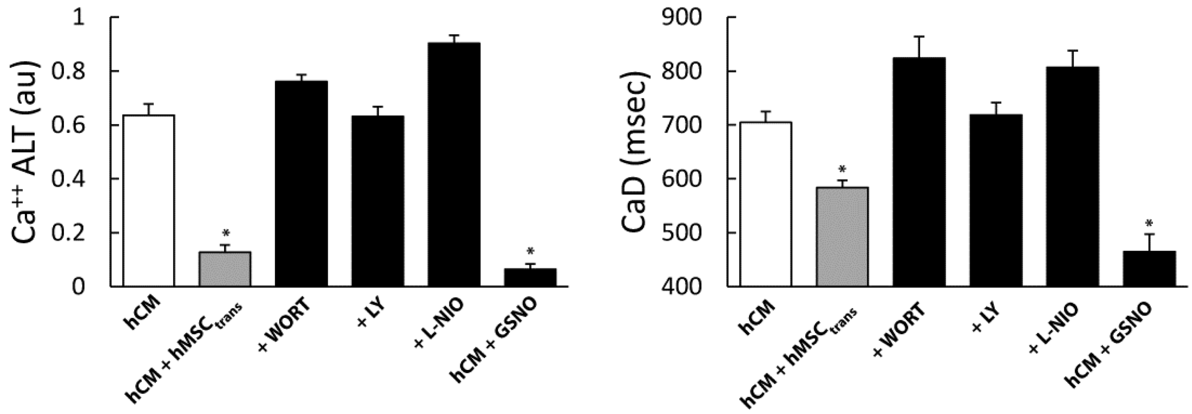

Figure 7.

The effects of PI3K inhibitors (Wortmannin, LY294002), eNOS inhibitor and no donor GSNO under conditions of oxidative stress. Graphs show summary data of Ca^{++} ALT (left) and CaD (right) for hCM alone, hCM+hMSC$_{trans}$, hCM+hMSC$_{trans}$+Wortmannin (+WORT), hCM+hMSC$_{trans}$+LY294002 (+LY), hCM+hMSC$_{trans}$+eNOS inhibitor (+L-NIO) and hCM +GSNO. PI3K and eNOS inhibitors significantly increased Ca^{++} ALT (n=8, $p< 0.0001$) and CaD (n=8, $p< 0.0001$). In contrast, Ca^{++} ALT (n=6, $p< 0.0001$) and CaD (n=6, $p< 0.0001$) were significantly decreased by GSNO in absence of hMSC. This suggests a mechanism of action related to PI3K mediated nitroso-redox pathway.

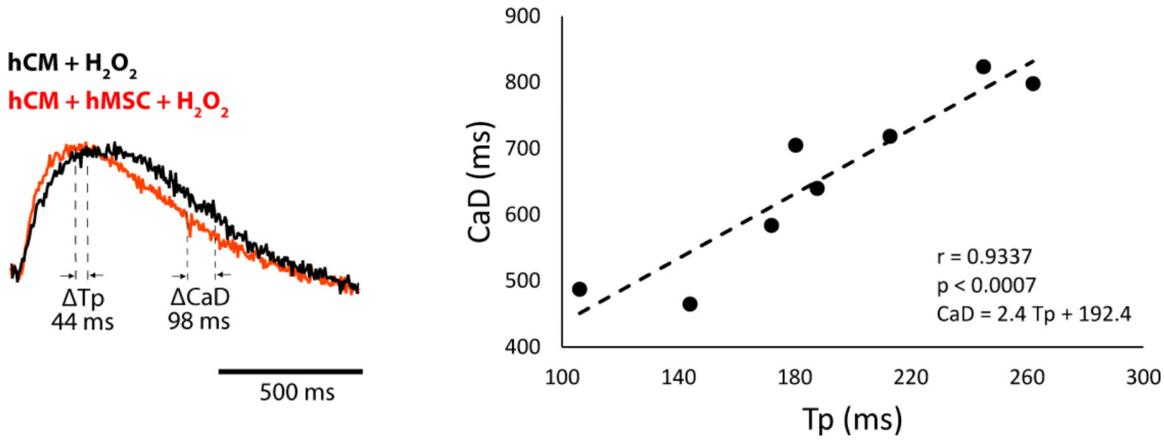

Figure 8.

Effects of hMSC on Tp and CaD. The Ca^{++} transients (left) recorded while pacing at a CL of 1200 msec show that compared to hCM alone (black) hMSC (red) decreased CaD more than Tp. The graph (right) shows a significant positive correlation between Tp and CaD with a slope of 2.4 (n=7, $p < 0.003$) measured under all conditions.